Clinical Neurophysiology 125 (2014) 2372–2383

Contents lists available at ScienceDirect

Clinical Neurophysiology

journal homepage: www.elsevier.com/locate/clinph

An automated and fast approach to detect single-trial visual evoked potentials with application to brain–computer interface

Yiheng Tu [a], Yeung Sam Hung [a], Li Hu [b], Gan Huang [a], Yong Hu [c], Zhiguo Zhang [a,*]

[a] Department of Electrical and Electronic Engineering, The University of Hong Kong, Pokfulam Road, Hong Kong, China
[b] Key Laboratory of Cognition and Personality (Ministry of Education), School of Psychology, Southwest University, Chongqing, China
[c] Department of Orthopaedics and Traumatology, The University of Hong Kong, Pokfulam Road, Hong Kong, China

ARTICLE INFO

Article history:
Accepted 18 March 2014
Available online 13 April 2014

Keywords:
Visual evoked potentials
Single-trial detection
Brain–computer interface
Wavelet analysis
Common spatial filtering

HIGHLIGHTS

- A joint spatial–temporal–spectral filter combining common spatial pattern and wavelet filtering can significantly increase the signal-to-noise ratio of single-trial visual evoked potentials.
- The proposed approach can obtain robust and reliable visual evoked potentials in an automated and fast manner, thus satisfying the requirements of practical brain–computer interface systems.
- The proposed approach can be potentially used to achieve real-time and automated detection of single-trial evoked potentials or event-related potentials in various paradigms.

ABSTRACT

Objective: This study aims (1) to develop an automated and fast approach for detecting visual evoked potentials (VEPs) in single trials and (2) to apply the single-trial VEP detection approach in designing a real-time and high-performance brain–computer interface (BCI) system.
Methods: The single-trial VEP detection approach uses common spatial pattern (CSP) as a spatial filter and wavelet filtering (WF) a temporal–spectral filter to jointly enhance the signal-to-noise ratio (SNR) of single-trial VEPs. The performance of the joint spatial–temporal–spectral filtering approach was assessed in a four-command VEP-based BCI system.
Results: The offline classification accuracy of the BCI system was significantly improved from 67.6 ± 12.5% (raw data) to 97.3 ± 2.1% (data filtered by CSP and WF). The proposed approach was successfully implemented in an online BCI system, where subjects could make 20 decisions in one minute with classification accuracy of 90%.
Conclusions: The proposed single-trial detection approach is able to obtain robust and reliable VEP waveform in an automatic and fast way and it is applicable in VEP based online BCI systems.
Significance: This approach provides a real-time and automated solution for single-trial detection of evoked potentials or event-related potentials (EPs/ERPs) in various paradigms, which could benefit many applications such as BCI and intraoperative monitoring.

1. Introduction

Brain–computer interface (BCI) is an emerging technology which can establish a pathway between the human brain and computers through recording and decoding brain activity (Wolpaw et al., 2002). Since the control of BCI system is directly based on the recorded brain activity without the involvement of neuromuscular system, it allows people who suffer from motor dysfunction or impairment (e.g., amyotrophic lateral sclerosis, brainstem stroke, and spinal cord injury) to communicate with the external world or control prosthesis (Vaughan et al., 2003). In addition, BCI plays an important role in neurofeedback training (Strehl et al., 2006), and can be used by healthy people in various applications, such as computer game control (Hjelm and Browall, 2000; Lalor et al., 2005) and music generation (Miranda, 2010).

* Corresponding author. Tel.: +852 22194577; fax: +852 25598738.
E-mail address: zgzhang@eee.hku.hk (Z. Zhang).

http://dx.doi.org/10.1016/j.clinph.2014.03.028
1388-2457/

Most existing BCI systems use electroencephalogram (EEG) to capture information on the subject's intention for controlling external devices (Niedermeyer and Da Silva, 2005). Visual evoked potentials (VEPs), which are phase-locked EEG responses evoked by visual stimulation, are one of the most extensively used EEG signals in BCI systems (Bin et al., 2009). According to the stimulus sequence modulation approach used, VEP-based BCI systems can be categorized into three types: (1) time modulated VEP (t-VEP) BCI, where stimulus sequences of different targets have independent and random flash onsets (Guo et al., 2008; Lee et al., 2006, 2008); (2) frequency modulated VEP (f-VEP) BCI, where stimuli are flashed at different frequencies (Allison et al., 2008; Jia et al., 2007; Middendorf et al., 2000; Müller-Putz et al., 2005); (3) code modulated VEP (c-VEP) BCI, where stimuli are encoded in pseudo-random binary sequences (Hanagata and Momose, 2002).

Recently, we have proposed a new encoding/decoding scheme for BCI based on chromatic transient VEP (CTVEP), which is evoked by low-frequency isoluminant chromatic stimuli for the purpose of minimizing the risk of eliciting epileptic seizures and reducing visual fatigue (Lai et al., 2011). In the CTVEP-BCI system, isoluminant chromatic stimuli are time-encoded into different binary codes ("1": presence of a visual stimulation; "0": absence of a visual stimulation), which are flickered simultaneously in different positions on the screen to serve as different input commands. Users can operate the BCI system by gazing at the target visual stimulation, and the user's intention can be decoded by calculating and comparing correlation coefficients between the code modulated CTVEP signals and CTVEP templates of different binary codes. Because the low-amplitude CTVEPs are usually buried in high-amplitude background of ongoing EEG and other non-cortical artifacts (Hu et al., 2010), the signal-to-noise ratio (SNR) of single-trial CTVEPs is very low, and reliable code-modulated CTVEPs were obtained by averaging EEG recordings of three identical epochs (Lai et al., 2011). This averaging approach could markedly enhance the SNR of CTVEPs, but greatly reduced the speed of the CTVEP-BCI system.

To achieve a high-speed and high-accuracy VEP-based BCI system, a fast and reliable approach to detect VEPs in single trials is highly desirable. Spatial filtering, which separates stimulus-elicited brain responses (e.g., VEPs) and ongoing EEG activity (or non-cortical artifacts) based on their distinct scalp distributions, has been popularly adopted to enhance the SNR of evoked potentials (EPs) and event-related potentials (ERPs) (Hu et al., 2011). One dominant spatial filter used is independent component analysis (ICA) (Makeig et al., 1996, 1997), which can identify and remove non-cortical artifacts, such as electrical activities related to eye blinks, eye movements, and muscle movements. In addition, temporal–spectral filtering, such as discrete wavelet filter (Quian Quiroga and Garcia, 2003) and continuous wavelet filter (Hu et al., 2010), can provide a time-varying filter based on time–frequency patterns of single-trial EPs/ERPs.

However, to the best of our knowledge, few single-trial EP/ERP detection methods have been successfully applied to real-time BCI systems for the following reasons. First, most available single-trial EP/ERP detection approaches are computationally demanding. Second, some techniques used for single-trial EP/ERP detection need intensive manual operation and cannot be executed automatically. Third, some spatial filtering techniques (such as ICA) only perform well on high-density EEG recordings (e.g., >16 channels), while a few-channel montage is more favored in practical BCI systems (Blankertz et al., 2011). To address these problems, we proposed an optimal filter by jointly utilizing distinct characteristics of VEPs in spatial, temporal, and spectral domains. This joint spatial–temporal–spectral filter was achieved by combining a common spatial pattern (CSP) based spatial filter and a wavelet filtering (WF) based temporal–spectral filter (Hu et al., 2010). The performance of the proposed spatial–temporal–spectral filter was evaluated by means of the SNR of single-trial CTVEPs, and the effectiveness of the proposed approach in the CTVEP-BCI system was assessed using classification accuracy. Furthermore, EEG data from fewer channels (i.e., 9, 7, and 5 channels) were used to evaluate the robustness of the single-trial VEP detection approach. Finally, the proposed approach was applied in a four-command VEP-based real-time BCI system, and its performance was evaluated in terms of information transfer rate.

2. Methods

2.1. Experimental design and EEG data collection

Eight healthy subjects (four males and four females) aged 21–25 years participated in the study. All subjects had normal or corrected-to-normal vision of $\geqslant$20/20 Snellen visual acuity, and were classified as normal color vision by the Ishihara test and the Farnsworth-Munsell 100-Hue test. No previous ocular or systemic disease was reported for these subjects. All subjects gave their written informed consent, and the local ethics committee approved the experimental procedures.

In each experiment, the subject was seated in a comfortable chair in a dim and unshielded laboratory with reasonable activities to simulate real-life situation. EEG signals were recorded using 13 Ag/AgCl channels positioned around the visual cortex based on the NeuroScan Quik-cap electrode placement system (Compumedics NeuroScan, EI Paso, TX, USA) with bandpass filtering of 1–30 Hz and a sampling rate of 1 kHz. Channels *Fz* and *Cz* were respectively used as ground and reference, and impedances of all channels were kept below 10 kΩ.

2.1.1. Offline BCI experiment

In the offline experiment (Fig. 1), subjects were instructed to gaze at the stimuli binocularly, and the viewing distance was 100 cm. Isoluminant red-green circular sinusoidal gratings with spatial frequency of 2 cpd were presented on a Dell 17.3″ HD + Anti-Glare LED-backlit monitor (Dell, Round Rock, TX, USA). The monitor's refreshing rate was 60 Hz, and the resolution of the screen was 1600 × 900 pixels (equivalent to 22° × 12°). In the CIE XYZ coordinate system, red was defined as $x = 0.406$, $y = 0.287$; green was defined as $x = 0.223$, $y = 0.374$. Their mean was $x = 0.314$, $y = 0.330$ with a mean luminance of 20 cd/m^2. Note that (x, y) represented the chromaticity coordinate in CIE 1931 XYZ color space, and the background was kept unchanged at the mean chromaticity and luminance. The stimulus had a diameter of 2° with a small black dot acting as the fixation center. Our previous study showed that such a configuration of visual stimulation could maximize the amplitude of CTVEPs (Lai et al., 2011). Chromatic stimuli were presented in a pattern onset/offset configuration. Precisely, a visual stimulus presented for 50 ms and then absented for 200 ms denoted the "1" bit, while one silent cycle without any visual stimulus for 250 ms denoted the "0" bit. We encoded the visual stimulation into six 4-bit binary codes, each containing two "1"-bits and two "0"-bits (1–1–0–0, 1–0–1–0, 0–1–0–1, 1–0–0–1, 0–0–1–1, 0–1–1–0), for these codes achieve a good tradeoff between the number of control inputs and the quality of input signals (Lai et al., 2011). In this study, four codes (1–1–0–0, 1–0–1–0, 0–1–0–1, 0–1–1–0) were used in the four-command BCI system (Fig. 1).

The offline experiment consisted of two sessions: a training session and a test session. The training session was used to obtain CTVEP templates for each subject, and the test session was used to validate the performance of the proposed spatial–temporal–spectral filter. In the training session, 20 segments of visual stimuli,

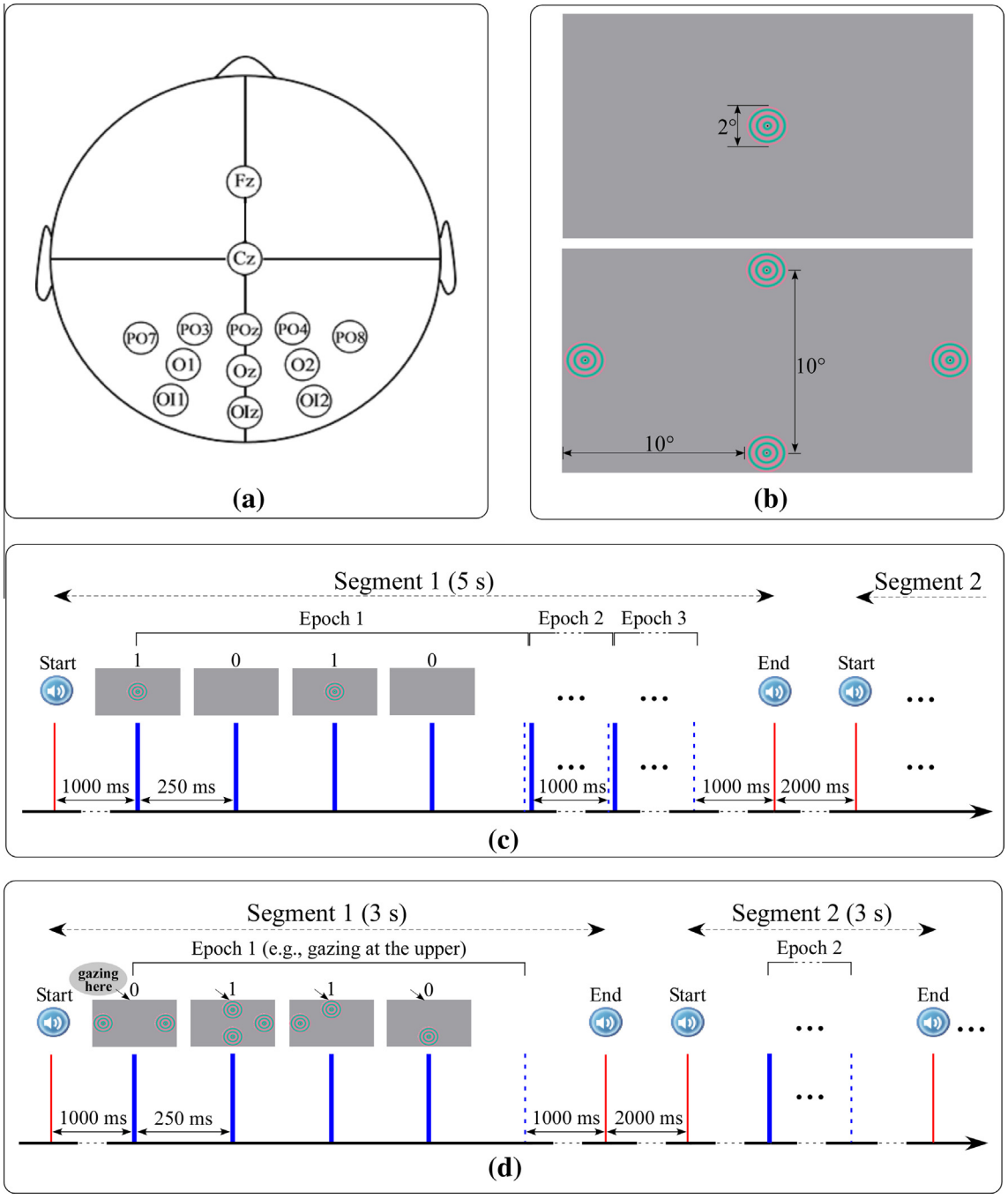

Fig. 1. Experiment design. (a) Channel montage used in the experiment. EEG data were collected from eleven channels over the visual cortex. Fz and Cz were respectively used as the ground and reference channels. (b) The locations of CTVEP stimuli (isoluminant red-green circular sinusoidal gratings with spatial frequency of 2 cpd) in training and test sessions were respectively displayed in the upper and lower panels. (c) The paradigm of the training session. Subjects were instructed to gaze at the fixation between the first and the second notification sounds to minimize eye blink. Visual stimuli were delivered in segments of three identical time-encoded epochs (4-bit code). A visual stimulus presented for 50 ms and then absented for 200 ms denoted the "1" bit, while one silent cycle without any visual stimulus for 250 ms denoted the "0" bit. Four types of 4-bit codes were randomly delivered at the center of the screen, and EEG data from in a total twenty segments (five segments per code) were collected. (d) The paradigm of the test session. The stimuli of four types of 4-bit codes were flickered simultaneously epoch by epoch with an inter-segment interval of 2 s in different locations of the screen (i.e., top, bottom, left, and right sides of the screen). (For interpretation of the references to colour in this figure legend, the reader is referred to the web version of this article.)

consisting of three identical time-encoded epochs (4-bit codes), were randomly presented at the center of the screen. The time interval between two consecutive segments was 2 s. Because two "1"-bit CTVEP trials were included in each time-encoded epoch, there were 60 epochs (20 segments × 3 epochs) and 120 "1"-bit CTVEP trials (60 epochs × 2 "1"-bit trials) in total in the training session. In the test session, the visual stimuli of the four types of 4-bit codes were flickered simultaneously in different locations of the screen (i.e., top, bottom, left, and right sides of the screen). Each segment contained only one epoch, and the time interval between consecutive segments was 2 s. Subjects were asked to gaze at the visual stimuli epoch by epoch in a clockwise order starting from the top side. In total, 20 CTVEP epochs (5 epochs per code) and 40 "1"-bit CTVEP trials (20 epochs × 2 "1"-bit trials) were collected in the test session (Fig. 1). It is important to note that, in this paper, an "epoch" denotes the EEG response to a 4-bit code and has a length of 1 s, while a "trial" denotes the EEG response to one bit ("1" or "0") and has a length of 250 ms.

2.1.2. Online BCI experiment

In the online experiment, subjects were instructed to play a mind-controlled Sokoban game, in which the game character was required to push crates to pre-specified storage locations. EEG signals were recorded and processed in real time by the proposed single-trial VEP detection approach. Details of the online game environment are introduced in Section 1 of the Supplementary Material.

2.2. Data analysis: single-trial VEP feature extraction

A novel spatial–temporal–spectral filter based on CSP (to filter the signal in the spatial domain) and WF (to filter the signal in the temporal–spectral domain) was developed for single-trial detection of CTVEPs. CSP can enhance the SNR of CTVEPs by separating and retrieving stimulus-evoked EEG responses from spontaneous EEG activity. WF is able to further enhance the SNR of CTVEPs by identifying and retaining the time–frequency pattern of CTVEPs matching that of the "1"-bit template.

2.2.1. Common spatial pattern

CSP was originally applied in EEG studies to quantitatively extract abnormal components from background EEG (Koles, 1991; Koles et al., 1990). Blankertz et al. (2008) showed that CSP could serve as a powerful technique in BCI for discriminating EEG signals with different mental intentions, and since then CSP has gradually gained popularity in BCI research. Because we encoded the visual stimuli into binary codes, i.e., "0" and "1" bits, CSP could be used to discriminate CTVEPs ("1"-bit) and resting EEG ("0"-bit) by regarding them as two different classes and maximizing the difference between the variances of the two classes.

Denote $\boldsymbol{X}_1^i \in \boldsymbol{R}^{N\times T}$ as the data of the ith "1"-bit, where N is the number of channels and T is the number of samples (in the present study $T = 250$ and $N = 11$ when all EEG channels were used). Similarly, denote $\boldsymbol{X}_0^i \in \boldsymbol{R}^{N\times T}$ as the data of the ith "0"-bit. CSP calculates the generalized eigenvector $\boldsymbol{w}$, which maximizes the difference in variance between two classes $\boldsymbol{X}_1^i$ and $\boldsymbol{X}_0^i$, by solving the equation:

$$\langle \boldsymbol{X}_1^i (\boldsymbol{X}_1^i)^T \rangle \boldsymbol{w} = \lambda \langle \boldsymbol{X}_0^i (\boldsymbol{X}_0^i)^T \rangle \boldsymbol{w} \quad (1)$$

where $\langle\cdot\rangle$ is the averaging operator and λ is the generalized eigenvalue. The matrix $\boldsymbol{W} = [\boldsymbol{w}_1, \ldots, \boldsymbol{w}_N] \in \boldsymbol{R}^{N\times N}$ consists of N eigenvectors, $\boldsymbol{w}_1, \ldots, \boldsymbol{w}_N$, estimated from Eq. (1), and $\mathbf{A} = \boldsymbol{W}^{-1} \in \mathbf{R}^{N\times N}$ is the spatial pattern represented as a weighting matrix of EEG channels. By sorting the eigenvalues, CSP provides an ordered list of spatial patterns according to their discriminative power between the two classes. The spatial pattern with the maximum variance of CTVEP-related components ($\boldsymbol{X}_1^i$) will capture the minimal variance of resting EEG-related components ($\boldsymbol{X}_0^i$). Typically, only a few pairs of spatial patterns can effectively discriminate between the two classes (Müller-Gerking et al., 1999). In this work, two spatial patterns (two eigenvectors corresponding to the largest and smallest eigenvalues) were selected to reconstruct spatial-filtered single-trial EEG responses of all channels (see Section 2 in the Supplementary Material for the reason of selecting two CSP components). These two spatial patterns, which isolated CTVEPs (contained only in $\boldsymbol{X}_1^i$) from spontaneous EEG (contained in $\boldsymbol{X}_0^i$ as well as in $\boldsymbol{X}_1^i$), worked as an effective spatial filter. The CSP-based spatial filter was modeled using EEG data collected in the training session, and was applied to EEG data collected in the test session.

In our previous work (Lai et al., 2011), spatial filtering was achieved by re-referencing EEG signals to Oz. Such a re-reference (Re-Ref) operation can suppress spontaneous EEG activities that had similar amplitudes widely spreaded over the visual cortex. Here, the performance (assessed using classification accuracy) of both spatial filters (CSP vs. Re-Ref) was compared.

2.2.2. Wavelet filtering

WF was used to isolate phase-locked CTVEPs from EEG artifacts in the time–frequency domain in the following steps (Fig. 2): (1) single-trial CTVEPs were transformed into time–frequency representations using continuous wavelet transform (CWT); (2) a specific time–frequency region (a mask for WF) representing power distribution of phase-locked CTVEPs was identified from the CWT of the averaged CTVEPs; (3) single-trial filtered CTVEPs were reconstructed from the wavelet coefficients within the CTVEP-related mask using inverse CWT (ICWT). The mask for WF was obtained from EEG signals collected in the training session, and applied to EEG signals collected in both the training and test sessions.

2.2.2.1. Continuous wavelet transform. CWT is able to obtain the time–frequency representation of a signal with an optimal compromise between time resolution and frequency resolution by adapting the temporal window width as a function of frequency. The CWT of one trial of CTVEP waveform $x(t)$ was obtained as:

$$W(\tau,f) = \int_t x(t)\sqrt{f/f_0}\psi^*(f/f_0(t-\tau))dt \quad (2)$$

$$\psi(t) = \frac{1}{\sqrt{\pi f_0}} e^{2i\pi f_0 t} e^{-\frac{t^2}{f_b}} \quad (3)$$

where τ and f are the time samples and frequency index respectively, and $\psi(t)$ is the Morlet wavelet acting as mother wavelet with central frequency f_0 and bandwidth f_b. In this study, f_b was set to 0.1, while f_0 was selected by an empirical function:

$$f_0 = 8.8P_{LF} - 3.52 \quad (4)$$

where P_{LF} was the power ratio of low frequency (<10 Hz) components of $x(t)$. The empirical function implied that f_0 was proportional to the low-frequency power of CTVEPs to be analyzed (see Section 3 of the Supplementary Material for details).

2.2.2.2. Time–frequency masking. A binary time–frequency mask M_f was generated from the CTVEP waveform averaged across all trials of one subject in the training session. The cumulative distribution function (CDF) of the time–frequency representation of the averaged CTVEP waveform was calculated. Where the CDF was larger than the threshold $0.55 \times [\max(\mathrm{CDF}) - \min(\mathrm{CDF})] + \min(\mathrm{CDF})$, the corresponding time–frequency pixels were set to 1, while others were set to 0. The threshold was determined with the objective of retaining the major feature of CTVEPs while removing as much noise as possible. In the present study, the threshold value was selected to achieve the highest classification accuracy in the training dataset (see Section 4 of the Supplementary Material). The filtered time–frequency representation WF of one trial was given by:

$$WF(\tau,f) = M_f W(\tau,f). \quad (5)$$

2.2.2.3. Inverse continuous wavelet transform (ICWT). Finally, the filtered single-trial CTVEP was obtained from the masked time–frequency representations using ICWT:

$$y(t) = \int_\tau \int_f (f/f_0)^2 WF(\tau,f)\sqrt{f/f_0}\psi(f/f_0(t-\tau))d\tau df \quad (6)$$

where $y(t)$ is the filtered single-trial CTVEP.

2.3. Performance evaluation

In order to quantitatively assess the performance of the proposed spatial–temporal–spectral filter, a similarity index (SMI) (Su et al., 2012), which was the power ratio between the

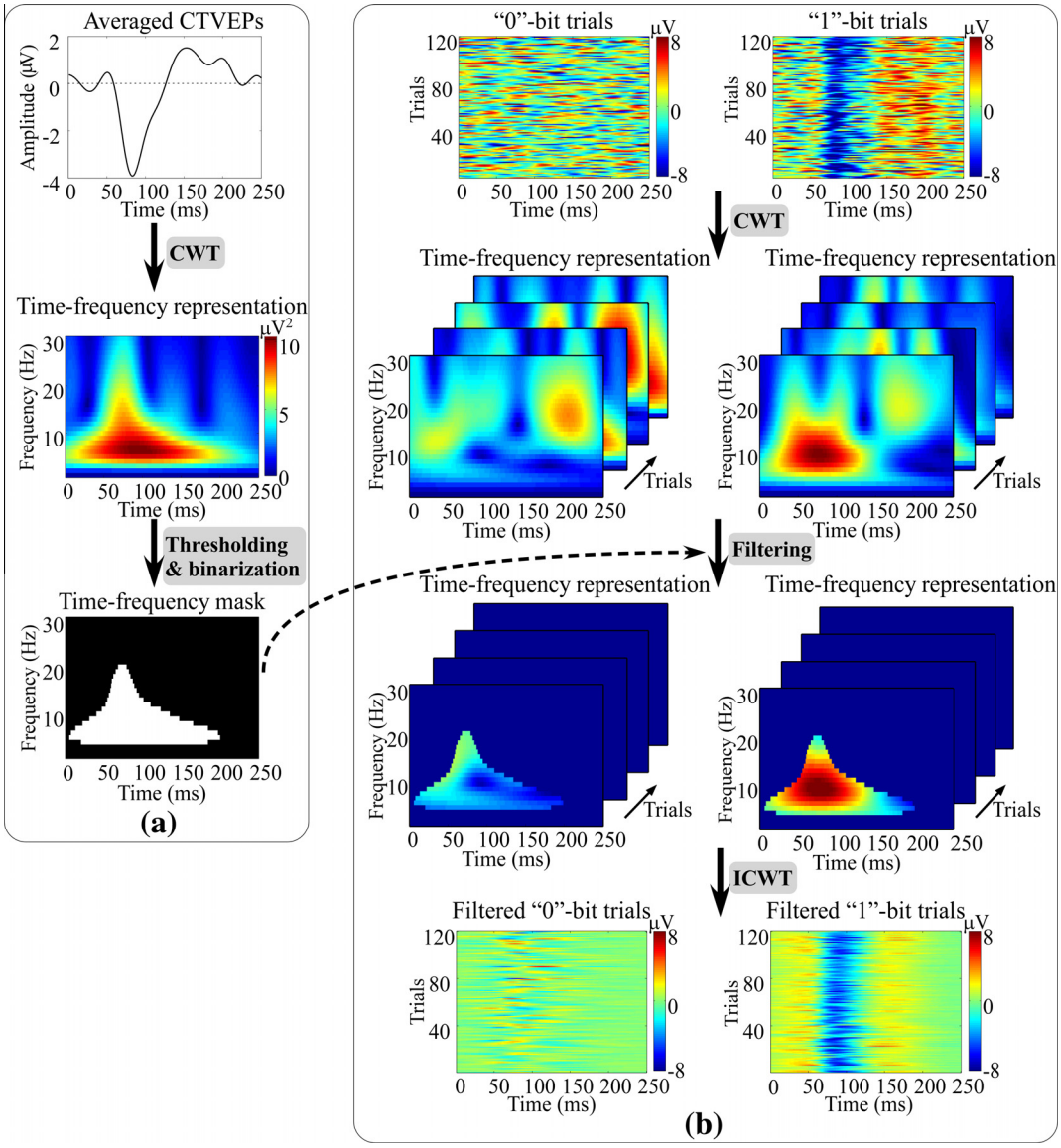

Fig. 2. Flowchart describing the procedure of WF to enhance the SNR of CTVEP responses. (a) The time–frequency representation of averaged CTVEPs was obtained using CWT, and the time–frequency mask was generated by thresholding this time–frequency representation. (b) The time–frequency mask was applied to single-trial time–frequency representations of both CTVEPs ("1"-bit) and resting EEG ("0"-bit). Filtered single-trial time-course data of both CTVEPs and resting EEG were reconstructed in the time domain using ICWT.

"CTVEP-like" signal in a test trial and the residual, was employed. Let $\overline{\boldsymbol{X}_1}$ be the average of all training trials of "1"-bit and $\boldsymbol{X}_1^i$ be the i^{th} test trial of "1"-bit. Then, the SMI was calculated as:

$$\mathrm{SMI} = 10\log_{10}(\sigma^2(\boldsymbol{S})/\sigma^2(\boldsymbol{N})) \tag{7}$$

where $\boldsymbol{S} = \frac{(\overline{\boldsymbol{X}_1})^T \boldsymbol{X}_1^i}{(\overline{\boldsymbol{X}_1})^T \overline{\boldsymbol{X}_1}} \overline{\boldsymbol{X}_1}$ is the orthogonal projection of $\boldsymbol{X}_1^i$ onto $\overline{\boldsymbol{X}_1}$, and $\boldsymbol{N} = \boldsymbol{X}_1^i - \boldsymbol{S}$ is the residual part. A large SMI implies that the test trial $\boldsymbol{X}_1^i$ is similar to the average $\overline{\boldsymbol{X}_1}$ of training trials. Thus, SMI can be used to approximate the SNR of single-trial CTVEPs (Huang et al., 2013).

SMI values calculated from the raw data, filtered data after CSP, and after CSP + WF were compared using a 3-level one-way repeated-measures analysis of variance (ANOVA). If the main effect of ANOVA was significant ($p < 0.05$), post hoc pairwise comparisons (two-sample t-test) were performed.

2.4. Feature extraction and classification

The Pearson's correlation method (PCM) (Rodgers and Nicewander, 1988) was used in our BCI system to classify the coded CTVEP epochs into four categories. Precisely, four CTVEP templates corresponding to four different binary codes were obtained in the training session. For each epoch in the test session, correlation coefficients between the current epoch and the four templates were calculated and compared. The epoch was classified into the category whose CTVEP template had the largest correlation coefficient with the epoch.

It should be noted that the PCM worked at the level of epochs instead of trials (one epoch consisted of four trials), and it was specific to the CTVEP-BCI system. To test whether the single-trial VEP detection approach contributes to single-trial classification, we used several classifiers, including support vector machine (Cortes and Vapnik, 1995; Kaper et al., 2004; Rakotomamonjy and Guigue, 2008), linear discriminant analysis (Bostanov, 2004; Garrett et al., 2003; Scherer et al., 2004), and Naïve Bayes (Zhang,

2004), to classify CTVEP waveforms (“1”-bit) and EEG activities (“0”-bit) based on extracted features (e.g., latency and amplitude). The results showed that each step of the single-trial VEP detection approach was able to significantly improve the accuracy of single-trial classification. Please refer to Section 5 of the Supplementary Material for details about classification based on latency and amplitude of VEP.

2.5. Performance assessment with fewer channel montages

Because a fewer channel montage is preferred in real BCI applications (Blankertz et al., 2011; Popescu et al., 2007), the performance of the proposed single-trial VEP detection approach was assessed (using classification accuracy) under nine settings of fewer-channel montages around the visual cortex (one 11-channel montage (I), two 9-channel montages (II and III), three 7-channel montages (IV, V, and VI), and three 5-channel montages (VII, VIII, and IX); see Fig. 3).

2.6. Performance assessment of online BCI system

The performance of the online BCI system was assessed using the information transfer rate (ITR):

$$\mathrm{ITR} = L \cdot \left[p\log_2(p) + (1-p)\log_2\left(\frac{1-p}{N-1}\right) + \log_2(N) \right] \tag{8}$$

where L is the number of decisions in one minute, and p is the accuracy of the subject in making decisions among N targets.

3. Results

3.1. CTVEP responses

Distinctive CTVEP responses (with two distinct deflections: a negative C_{II} deflection and a positive C_{III} deflection) were obtained at all channels and from all 8 subjects in the offline training session (Fig. 4), although there was large variability across channels and subjects. The latencies and amplitudes of averaged C_{II} and C_{III} at Oz were as follows: C_{II} latency (106.3 ± 21.9 ms); C_{II} amplitude (−4.2 ± 1.1 μV); C_{III} latency (194.1 ± 40.4 ms); C_{III} amplitude (3.7 ± 2.3 μV). Another positive C_I deflection, which is mainly responsible for isochromatic luminance modulation (Odom et al., 2004), was presented with a small amplitude, which was consistent with our previous work (Lai et al., 2011).

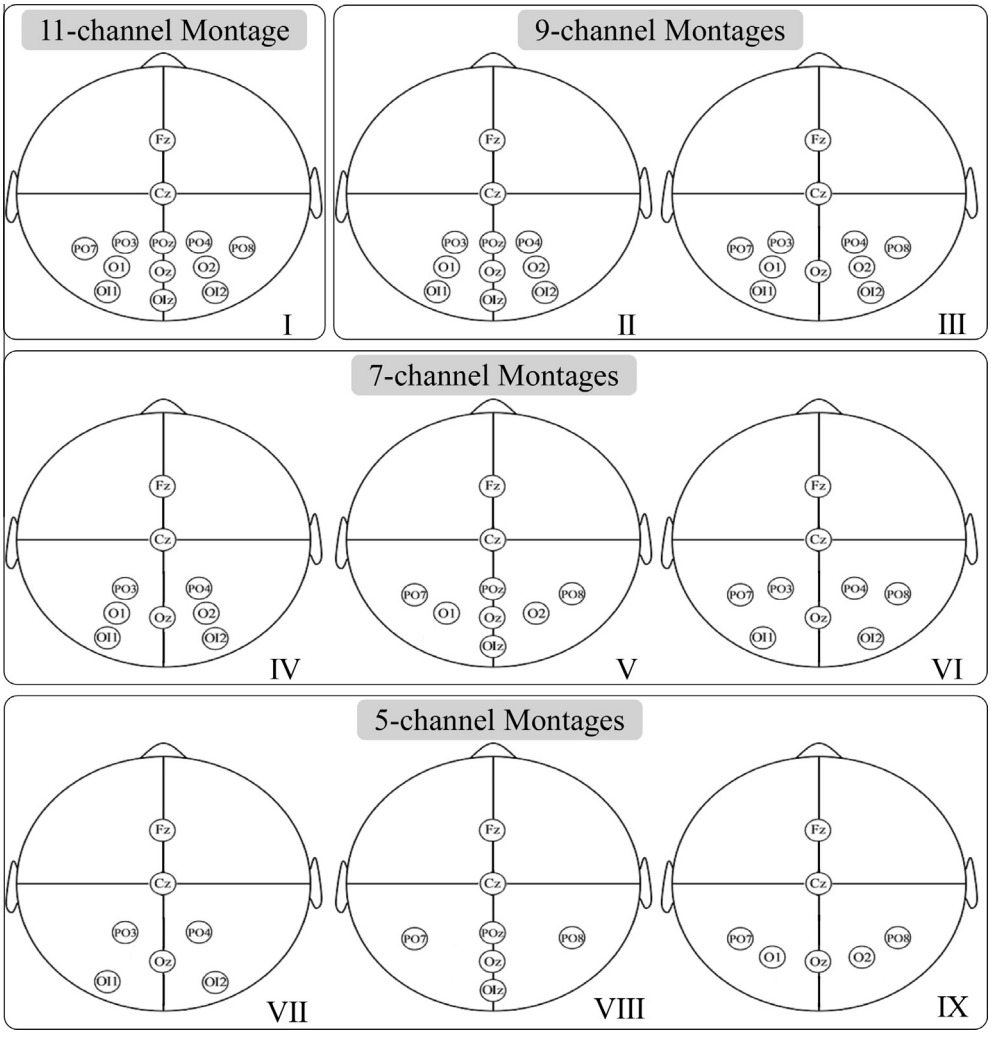

Fig. 3. Nine types of montages with fewer channels were used to evaluate the performance of the single-trial VEP detection approach, including one type of 11 channels (I), two types of 9 channels (II, III), three types of 7 channels (IV, V, VI), and three types of 5 channels (VII, VIII, IX). Note that the selected channels were close to Oz, where the strongest CTVEP responses were detected.

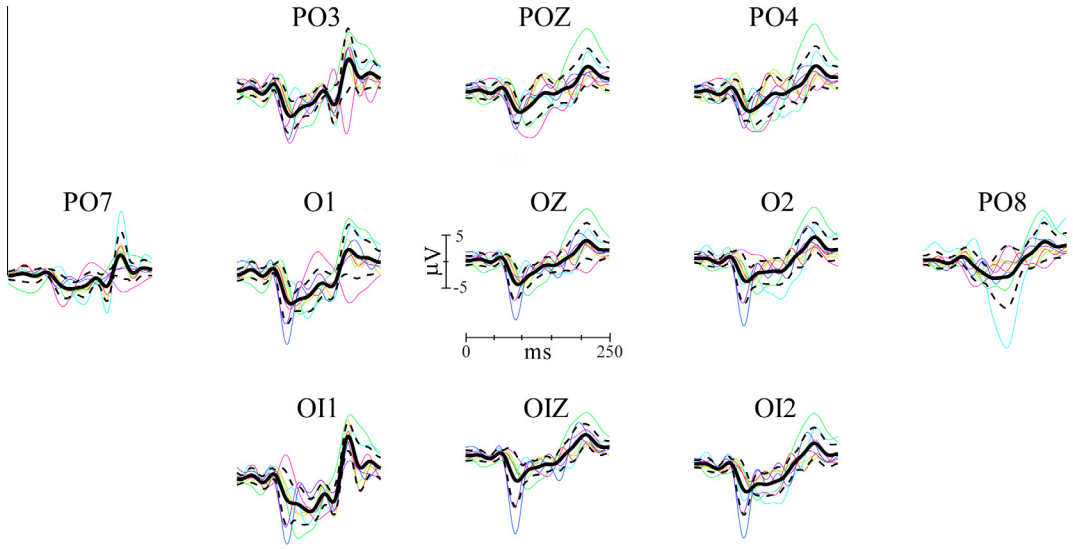

Fig. 4. Averaged CTVEP responses (raw data) of all channels. Colored lines denote the averaged CTVEP responses of each subject, and the bold and dash black lines denote respectively the group average and standard deviation of CTVEP responses across subjects. (For interpretation of the references to color in this figure legend, the reader is referred to the web version of this article.)

3.2. Performance of the spatial–temporal–spectral filter

Fig. 5 (a) showed the effect of each filtering step (CSP and WF) in the proposed spatial–temporal–spectral filter on "0"-bit trials and "1"-bit trials at Oz for a representative subject. Fig. 5 (b) demonstrated that both CSP and WF significantly enhanced the SMI of CTVEP trials (raw data: -6.44 ± 4.23; after CSP: 0.22 ± 3.95; after CSP + WF: 10.80 ± 6.18; $F = 37.79$, $p < 0.0001$; one-way repeated-measures ANOVA). Post hoc comparison revealed that the enhancements of SMI (1) from raw data to filtered data after CSP, (2) from raw data to filtered data after CSP + WF, and (3) from filtered data after CSP to filtered data after CSP + WF were significant ($p = 0.004$, $p < 0.001$, and $p < 0.001$ respectively; two-sample t-test).

3.3. Classification accuracy of offline BCI

Fig. 6 (a) showed the correlation coefficients between code-modulated CTVEP epochs and four CTVEP templates for a representative subject. Correlation coefficients between each epoch and their corresponding template (CC_C) were marked in red, while correlation coefficients between each epoch and mismatched templates (CC_M) were marked in other colors. Intuitively, a high classification accuracy required CC_C to be larger than the corresponding CC_M in most epochs. In the top row of Fig. 6 (a), CC_C obtained from raw data was not the largest among all four CC in most epochs, which indicated the classification accuracy was not high. In the middle row of Fig. 6 (a), CC_C obtained from filtered data after CSP was the largest among all four correlation coefficients in most epochs while the distance between CC_C and CC_M was small. In the bottom row of Fig. 6 (a), CC_C obtained from filtered data after CSP + WF was the largest among all four correlation coefficients in almost all epochs and the distance between CC_C and CC_M was larger, indicating higher classification accuracy.

Fig. 6 (b) illustrated the significant increase of classification accuracy across subjects after each step (raw data: $67.6 \pm 12.5\%$; data after Re-Ref: $78.3 \pm 7.1\%$; data after Re-Ref + WF: $85.6 \pm 9.0\%$; data after CSP: $88.4 \pm 6.2\%$; data after CSP + WF: $97.3 \pm 2.1\%$; $F = 26.14$, $p < 0.0001$; one-way repeated-measures ANOVA). Post hoc comparison revealed that the classification accuracy from data after CSP + WF was significantly higher than those from raw data, data after Re-Ref, data after Re-Ref + WF, and data after CSP ($p < 0.01$ for all comparisons; two-sample t-test).

3.4. Performance on fewer channel montages

Tables 1 and 2 respectively summarized the classification accuracy of each subject obtained from filtered data after CSP and data after CSP + WF using nine types of fewer-channel montages around the visual cortex (Fig. 3). Generally, the classification accuracy was decreased with the reduction of the channels, implying that the performance of CSP was limited by fewer-channel montages. In addition, the classification accuracy obtained from filtered data after CSP + WF was significantly larger than that from filtered data after CSP for all types of fewer channel montages ($p < 0.01$ for I and II; $p < 0.05$ for III, IV, VI, VII, and VIII), which indicated that the WF could compensate for the limited performance of CSP to some extent when fewer-channel montages were used.

3.5. Performance of online BCI system

All eight subjects were instructed to play the mind-controlled Sokoban game through the online CTVEP-BCI system, and all of them successfully operated the online BCI system. Specifically, subjects could make 20 decisions in one minute ($L = 20$) with an average accuracy of 90%. Thus, the ITR of the online CTVEP-BCI system was 27.5 bits/min. In addition, the proposed spatial–temporal–spectral filter and the PCM-based classification were computationally effective (<100 ms for one trial with PC configuration of *Intel Core i7–2600 CPU @ 3.40 GHz and 8 GB RAM*) so that they can be well used for online BCI systems.

4. Discussion

In this paper, an automated and fast single-trial VEP detection approach, which combined a CSP-based spatial filter and a WF-based temporal–spectral filter, was developed for a CTVEP-BCI system. Results obtained from an offline BCI system showed that the SNR of single-trial VEPs was significantly improved by using the proposed approach. The single-trial VEP detection approach can significantly increase the classification accuracy of a four-command offline CTVEP-BCI system from $67.6 \pm 12.5\%$ to $97.3 \pm 2.1\%$. Further, the proposed approach was successfully implemented in a four-command online CTVEP-BCI system, which worked accurately and effectively on normal subjects achieving an ITR of 27.5 bits/min.

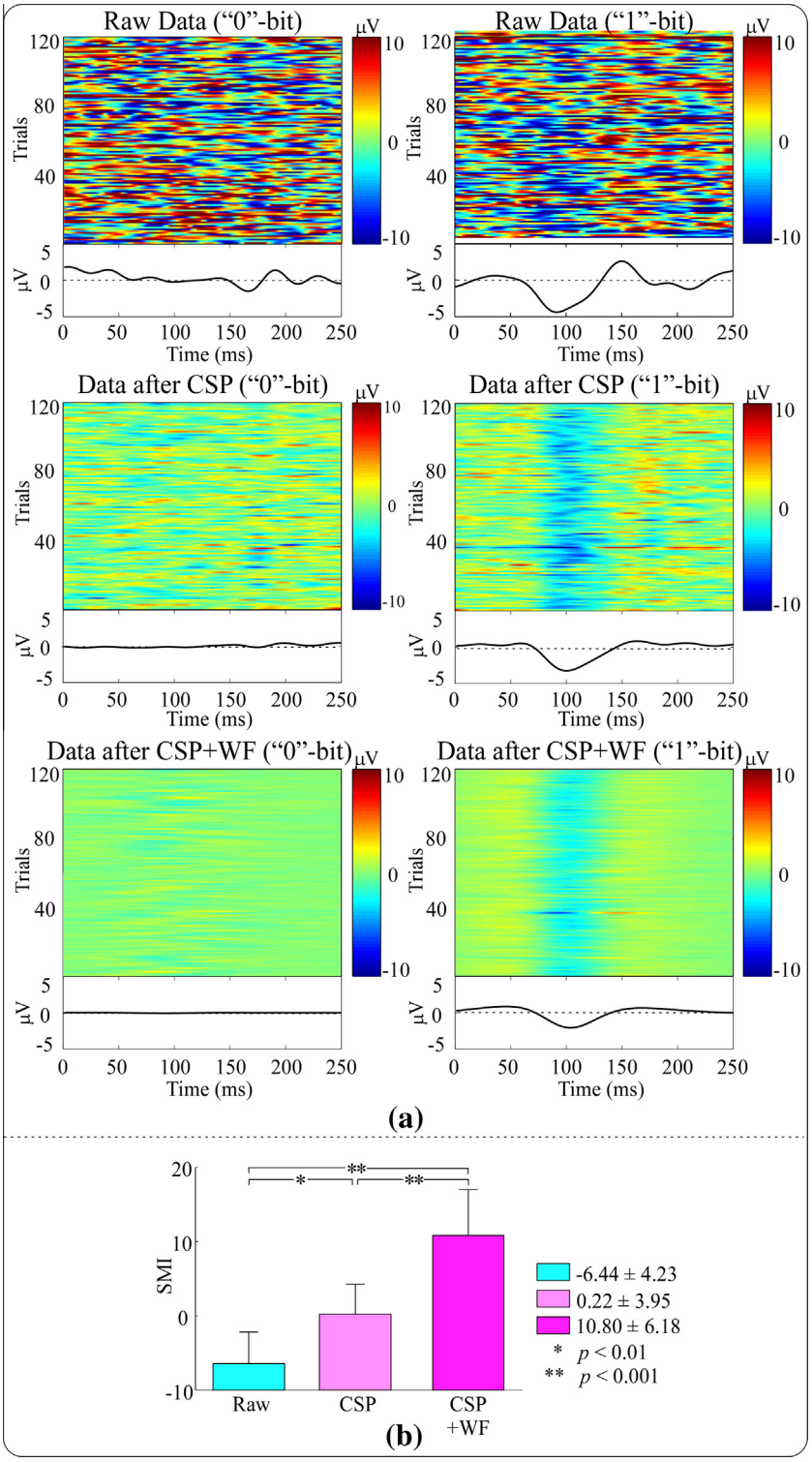

Fig. 5. Performance of the proposed single-trial VEP detection approach on CTVEP trials and resting EEG trials (measured at Oz). (a) One hundred and twenty single-trial CTVEPs and resting EEG from a representative subject were processed by CSP and WF. (b) The proposed single-trial VEP detection approach significantly enhanced the SMI of CTVEP responses (lower panel; $F = 37.79$, $p < 0.0001$; one-way repeated-measures ANOVA).

4.1. Methodological considerations

4.1.1. Spatial filter

Numerous spatial filter algorithms have been well developed to enhance the SNR of EP/ERPs and to improve the prediction accuracy in BCI systems (McFarland et al., 1997). Because of the capability of identifying and removing electrooculographical or electromyographical artifacts from EEG, ICA has been extensively used in BCI systems based on P300 (Xu et al., 2004), auditory EP (Hill et al., 2004), steady-state VEP (Wang et al., 2006), and motor imaginary EEG (Qin et al., 2004). However, it has been shown that the performance of ICA in isolating stimulus-evoked components was not satisfactory because ICA essentially attempts to find non-Gaussian components but EEG source components are often

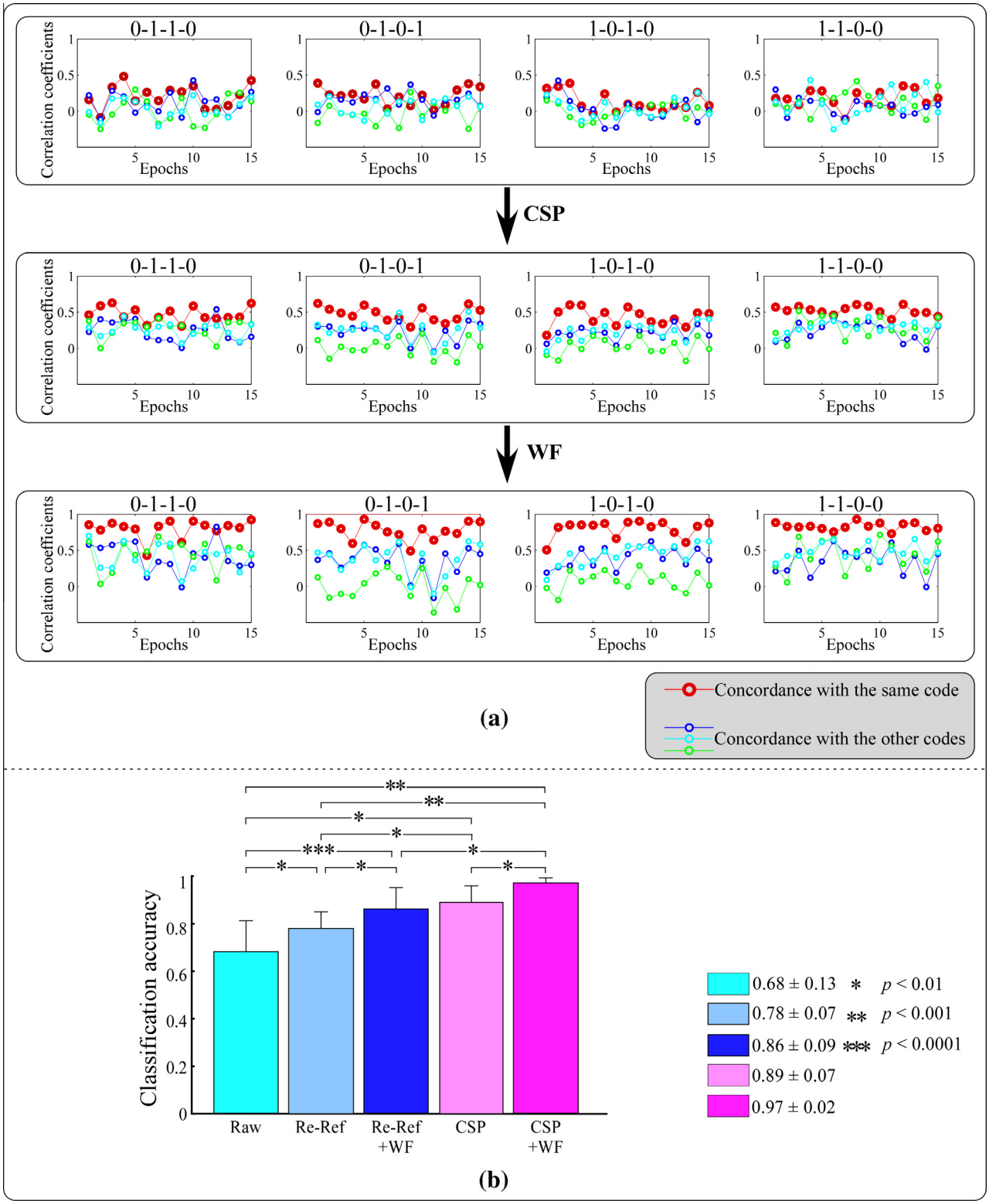

Fig. 6. Improvements of classification accuracy by the proposed single-trial detection approach. (a) Correlation coefficients between code modulated CTVEP epochs and four CTVEP templates from a representative subject. Red circles indicate correlation coefficients calculated between CTVEP epochs and their corresponding template (CC_C). Circles with other colors indicate correlation coefficients calculated between CTVEP epochs and mismatched templates (CC_M). (b) The proposed single-trial detection approach significantly improved the classification accuracy ($F = 26.14$, $p < 0.0001$; one-way repeated-measures ANOVA). Error bars represent standard deviation across subjects. (For interpretation of the references to color in this figure legend, the reader is referred to the web version of this article.)

not far from Gaussian (Hyvärinen et al., 2010). Therefore, ICA may not be able to effectively discriminate and isolate stimulus-related EEG responses from various artifacts.

In contrast, CSP, being a supervised algorithm that makes use of prior information on two populations of multivariate signals, decomposes EEG signals into a set of spatial patterns, which

Table 1
Classification accuracy obtained from data after CSP with montages of fewer channels.

Subjects	I	II	III	IV	V	VI	VII	VIII	IX
#1	0.87	0.80	0.70	0.57	0.75	0.82	0.78	0.42	0.73
#2	0.87	0.75	0.57	0.52	0.72	0.88	0.67	0.68	0.77
#3	0.98	0.80	0.52	0.52	0.98	0.95	0.62	0.32	0.78
#4	0.83	0.45	0.82	0.65	0.83	0.58	0.72	0.67	0.67
#5	0.90	0.90	0.75	0.77	0.93	0.58	0.82	0.62	0.92
#6	0.94	0.97	0.98	0.87	0.57	0.83	0.80	0.80	0.58
#7	0.78	0.82	1.00	1.00	0.93	0.77	0.92	0.55	0.50
#8	0.90	0.90	0.88	0.80	0.93	0.87	0.88	0.87	0.93
Mean	0.88	0.80	0.78	0.71	0.83	0.79	0.78	0.61	0.74
Std	0.06	0.16	0.18	0.18	0.14	0.14	0.10	0.18	0.15

Table 2
Classification accuracy obtained from data after CSP + WF with montages of fewer channels.

Subjects	I	II	III	IV	V	VI	VII	VIII	IX
#1	0.94	0.95	0.92	0.92	0.87	0.92	0.98	0.75	0.77
#2	0.95	0.92	0.63	0.80	0.77	0.92	0.85	0.77	0.78
#3	0.98	0.92	0.97	0.70	0.98	0.97	0.88	0.70	0.83
#4	0.97	0.55	0.92	0.68	0.93	0.63	0.73	0.75	0.70
#5	0.97	0.97	0.87	0.92	0.97	0.75	0.87	0.80	0.95
#6	1.00	1.00	1.00	0.98	0.95	0.98	0.97	0.78	0.87
#7	1.00	1.00	1.00	1.00	1.00	1.00	0.97	1.00	0.97
#8	0.97	0.91	0.91	0.87	0.93	0.89	0.89	0.81	0.86
Mean	0.97	0.91	0.91	0.87	0.93	0.89	0.90	0.81	0.86
Std	0.02	0.15	0.12	0.12	0.07	0.13	0.08	0.11	0.10

maximizes their difference in variance (Blankertz et al., 2008; Müller-Gerking et al., 1999). Importantly, the decomposed components obtained using CSP are ordered according to their discriminative powers. For this reason, unlike the selection of independent components which heavily relies on the experience of operators, the CSP components can be selected automatically based on their discriminative powers. Although CSP has been popularly used in motor-imagery BCI for detecting event-related synchronization or desynchronization (Blankertz et al., 2008; Müller-Gerking et al., 1999), its application for extracting EP waveforms has rarely been explored. In the present study, EEG data after visual stimuli and resting EEG data were regarded as two populations of multivariate signals in the CSP analysis. Since VEPs capture major difference between the two populations of EEG data, they can be well isolated from resting EEG by using CSP. In addition, CSP can be executed rapidly and therefore is suitable for BCI applications.

Visual stimuli will sometimes induce eye blinks and muscle activities, which cannot be identified and removed by CSP because these non-cortical activities also account for the difference between spontaneous activities and evoked responses. To address the problem, an improved CSP using local temporally neighboring samples can be applied to take into account the temporal information of non-cortical activities in the estimation of covariance since the outliers can only affect their neighboring samples (Wang and Zheng, 2008). Another variant of CSP, called common spatio-spectral pattern (CSSP) (Lemm et al., 2005), can also be used to improve the performance of CSP. CSSP embeds a finite impulse response spectral filter into CSP to produce a spatio-spectral filter. Since it simultaneously performs filtering in the spatial domain and the spectral domain, CSSP is expected to better discriminate evoked EEG responses than CSP.

4.1.2. Temporal–spectral filter

To further enhance the SNR of single-trial VEPs, especially when the number of EEG channels was limited, WF was adopted to analyze the CSP-filtered single-trial VEPs in the present study. WF was achieved by thresholding the time–frequency representation of group-averaged CTVEPs, with an aim to retain only the phase-locked CTVEPs. Compared with conventional filtering in the frequency domain, the temporal–spectral filter has time-varying filter coefficients, so that it is better suited to enhance the SNR of EPs/ERPs, whose spectrum varies greatly with time.

Many time–frequency analysis methods, such as the short-time Fourier transform, can be used in the temporal–spectral filtering. We chose CWT because it achieves an optimal compromise between time and frequency resolutions by adapting the temporal window width as a function of estimated frequency. Therefore, CWT is able to obtain clear representations of both low-frequency components and high-frequency components of the VEPs, facilitating subsequent temporal–spectral filtering. Our online BCI experiment also showed that the CWT-based temporal–spectral filtering could be implemented in real time.

4.2. Extensions of CTVEP BCI

In the proposed CTVEP-BCI system, a 4-bit coding scheme was adopted and only four (each of them consisted of two "1" bits) out of 16 possible codes were used to encode the control commands. Since the proposed single-trial VEP detection approach was applied to every bit of EEG signals, the CTVEP-BCI system could be easily extended in two aspects: (1) use more codes in the 4-bit coding scheme and (2) increase the number of bits in the coding scheme. Such an extended CTVEP-BCI system can be used for more complicated tasks that require more commands. It should however be noted that too many "1" bits should be avoided in a code, since CTVEPs can be suppressed due to repeated presentation of visual stimuli with short interstimulus interval (Lai et al., 2011).

4.3. Potential applications

4.3.1. Application to BCI

Single-trial detection of ERPs/EPs is crucial for ERP/EP-based BCI systems, and, therefore, the proposed approach can be potentially applied to various types of ERP/EP-based BCI systems, such as BCI based on t-VEP (Guo et al., 2008; Lee et al., 2008), c-VEP (Hanagata and Momose, 2002), and P300 (Krusienski et al., 2007; Pires et al., 2009). In all these BCI systems, the CSP-based spatial filter can be used to isolate components containing ERP/EP by defining EEG data before and after the presentation of stimulation as two populations of multivariate signals. Subsequently, the WF-based temporal–spectral filter can be adopted to further enhance the SNR of single-trial ERPs/EPs at each channel.

4.3.2. Application to neuroscience and clinical neurophysiology

Conventionally, the detection of ERPs/EPs relied on the across-trial averaging (Rugg and Coles, 1995), which assumes that ERPs/EPs are constant across trials. However, this assumption does not hold, since converging evidence show that ERPs/EPs are largely modulated by changes in stimulus parameters and cognitive fluctuations, which vary considerably from trial to trial (Hu et al., 2010; Mayhew et al., 2010; Mouraux and Iannetti, 2008). Therefore, it is beneficial to apply single-trial ERP/EP detection techniques in various fields of neuroscience and clinical neurophysiology to reveal trial-to-trial dynamics in electrophysiological recordings (Makeig et al., 2004). In addition, since the proposed approach does not require any manual intervention, it will not lead to any detection bias caused by subjective judgment and can relieve operators from laborious manipulations. Importantly, single-trial ERP/EP detection can serve as a key technology for integration of simultaneously-recorded EEG and functional magnetic resonance imaging signals (Bénar et al., 2007; Debener et al., 2006). By correlating trial-to-trial ERP/EP features with fMRI

responses, we can reveal brain responses that were elicited by any stimulus presentation or cognitive event with both high temporal and spatial resolutions. Also, the proposed single-trial detection approach can be applied in intra-operative neuro-monitoring to detect ERP/EP changes with the progressive of operation and to prevent any possible and potential neurologic damage (Hu et al., 2001; Luk et al., 2001; Thomusch et al., 2002).

In this study, the proposed single-trial EP/ERP detection method performed well at the within-subject level (i.e., the method was trained on and applied to the same subject). But in clinical neurophysiology, it is more desirable to detect single-trial EP/ERP waveforms at the between-subject level (i.e., the proposed method can be trained on a cohort of subjects and applied to another subject). We also tested the performance of the proposed method at the between-subject level using leave-one-subject-out cross-validation (see Section 6 in the Supplementary Material). It was shown that the single-trial EP/ERP detection approach can also significantly increase the classification accuracy at the between-subject level ($p = 0.01$, paired sample t-test) when all subjects have normal VEPs, but the accuracy at the between-subject level was not as high as that at the within-subject level due to the relatively large inter-subject variability. If the inter-subject variability is too large (for example, some subjects have too short latencies or prolonged latencies in VEPs), the proposed approach may not work well at the between-subject level. Lastly, the good performance of the proposed single-trial VEP detection approach is heavily dependent on the compatibility of the VEP template with the single-trial VEP response to be classified. When dealing with abnormal VEPs (which are often encountered in clinical applications), the proposed method can achieve satisfactory performance only if we can have a template of abnormal VEPs and the morphology of abnormal VEPs is consistent across trials (for within-subject classification) or across subjects (for between-subject variability).

Acknowledgements

ZZ is supported by the Seed Funding for Basic Research (201203159009) from HKU CRCG. YSH is supported by a Grant (HKU 762111M) from the Hong Kong SAR Research Grants Council. LH is supported by National Natural Science Foundation of China (No. 81271685). All authors have no conflict of interest.

Appendix A. Supplementary data

Supplementary data associated with this article can be found, in the online version, at http://dx.doi.org/10.1016/j.clinph.2014.03.028.

References

Allison BZ, McFarland DJ, Schalk G, Zheng SD, Jackson MM, Wolpaw JR. Towards an independent brain–computer interface using steady state visual evoked potentials. Clin Neurophysiol 2008;119:399.

Bénar CG, Schön D, Grimault S, Nazarian B, Burle B, Roth M, et al. Single-trial analysis of oddball event-related potentials in simultaneous EEG-fMRI. Hum Brain Mapp 2007;28:602–13.

Bin G, Gao X, Wang Y, Hong B, Gao S. VEP-based brain–computer interfaces: time, frequency, and code modulations [Research Frontier]. IEEE Comput Intell Mag 2009;4:22–6.

Blankertz B, Lemm S, Treder M, Haufe S, Müller K-R. Single-trial analysis and classification of ERP components – a tutorial. Neuroimage. 2011;56:814–25.

Blankertz B, Tomioka R, Lemm S, Kawanabe M, Muller K-R. Optimizing spatial filters for robust EEG single-trial analysis. IEEE Signal Process Mag. 2008;25:41–56.

Bostanov V. BCI competition 2003-data sets Ib and IIb: feature extraction from event-related brain potentials with the continuous wavelet transform and the t-value scalogram. IEEE Trans Biomed Eng. 2004;51:1057–61.

Cortes C, Vapnik V. Support-vector networks. Mach learn 1995;20:273–97.

Debener S, Ullsperger M, Siegel M, Engel AK. Single-trial EEG-fMRI reveals the dynamics of cognitive function. Trends Cogn Sci 2006;10:558–63.

Garrett D, Peterson DA, Anderson CW, Thaut MH. Comparison of linear, nonlinear, and feature selection methods for EEG signal classification. IEEE Trans Neural Syst Rehabil Eng 2003;11:141–4.

Guo F, Hong B, Gao X, Gao S. A brain–computer interface using motion-onset visual evoked potential. J Neural Eng 2008;5:477.

Hanagata J, Momose K. A method for detecting gazed target using visual evoked potentials elicited by pseudorandom stimuli. Proc 5th Asia Pacific Conf Medical and Biological Engineering and 11th Int Conf, Biomedical Engineering (ICBME)2002.

Hill NJ, Lal TN, Bierig K, Birbaumer N, Scholkopf B. Attention modulation of auditory event-related potentials in a brain–computer interface. In: 2004 IEEE International Workshop on Biomedical Circuits and Systems. IEEE; 2004. p. S3/5/INV-S3/17-20.

Hjelm SI, Browall C. Brainball-using brain activity for cool competition. In: Proceedings of NordiCHI; 2000. p. 177–88.

Hu L, Liang M, Mouraux A, Wise RG, Hu Y, Iannetti GD. Taking into account latency, amplitude and morphology: improved estimation of single-trial ERPs by wavelet filtering and multiple linear regression. J Neurophysiol 2011a;106:3216–29.

Hu L, Mouraux A, Hu Y, Iannetti G. A novel approach for enhancing the signal-to-noise ratio and detecting automatically event-related potentials (ERPs) in single trials. Neuroimage 2010;50:99–111.

Hu L, Zhang ZG, Hung YS, Luk KD, Iannetti GD, Hu Y. Single-trial detection of somatosensory evoked potentials by probabilistic independent component analysis and wavelet filtering. Clin Neurophysiol 2011b;122:1429–39.

Hu Y, Luk KD, Wong YW, Lu WW, Leong JC. Effect of stimulation parameters on intraoperative spinal cord evoked potential monitoring. J Spinal Disord Tech 2001;14:449–52.

Huang G, Xiao P, Hung YS, Zhang ZG, Hu L. A novel approach to predict subjective pain perception from single-trial laser-evoked potentials. Neuroimage 2013;81C:283–93.

Hyvärinen A, Ramkumar P, Parkkonen L, Hari R. Independent component analysis of short-time Fourier transforms for spontaneous EEG/MEG analysis. Neuroimage 2010;49:257–71.

Jia C, Xu H, Hong B, Gao X, Zhang Z, Gao S. A human computer interface using SSVEP-based BCI technology. Foundations of Augmented Cognition. 2007:113–9.

Kaper M, Meinicke P, Grossekathoefer U, Lingner T, Ritter H. BCI competition 2003-data set IIb: Support vector machines for the P300 speller paradigm. IEEE Trans Biomed Eng 2004;51:1073–6.

Koles ZJ. The quantitative extraction and topographic mapping of the abnormal components in the clinical EEG. Electroencephalogr Clin Neurophysiol 1991;79:440–7.

Koles ZJ, Lazar MS, Zhou SZ. Spatial patterns underlying population differences in the background EEG. Brain Topog 1990;2:275–84.

Krusienski D, Sellers E, Vaughan T. Common spatio-temporal patterns for the P300 speller. 2007 CNE'07 3rd international IEEE/EMBS conference on neural engineering. IEEE; 2007. p. 421–4.

Lai SM, Zhang Z, Hung YS, Niu Z, Chang C. A chromatic transient visual evoked potential based encoding/decoding approach for brain–computer interface. IEEE J Emerg Sel Topic Circuts Syst 2011;1:578–89.

Lalor E, Kelly S, Finucane C, Burke R, Reilly R, McDarby G. Brain computer interface based on the steady-state VEP for immersive gaming control. Eurasip J Adv Sig Pr 2005;19:3156–64.

Lee P-L, Hsieh J-C, Wu C-H, Shyu K-K, Chen S-S, Yeh T-C, et al. The brain computer interface using flash visual evoked potential and independent component analysis. Ann Biomed Eng 2006;34:1641–54.

Lee P-L, Hsieh J-C, Wu C-H, Shyu K-K, Wu Y-T. Brain computer interface using flash onset and offset visual evoked potentials. Clin Neurophysiol 2008;119:605–16.

Lemm S, Blankertz B, Curio G, Muller K-R. Spatio-spectral filters for improving the classification of single trial EEG. IEEE Trans Biomed Eng 2005;52:1541–8.

Luk KD, Hu Y, Lu WW, Wong Y. Effect of stimulus pulse duration on intraoperative somatosensory evoked potential (SEP) monitoring. J Spinal Disord Tech 2001;14:247–51.

Makeig S, Bell AJ, Jung T-P, Sejnowski TJ. Independent component analysis of electroencephalographic data. Adv Neural Inf Process Syst 1996:145–51.

Makeig S, Debener S, Onton J, Delorme A. Mining event-related brain dynamics. Trends Cogn Sci 2004;8:204–10.

Makeig S, Jung T-P, Bell AJ, Ghahremani D, Sejnowski TJ. Blind separation of auditory event-related brain responses into independent components. Proc Natl Acad Sci USA 1997;94:10979–84.

Mayhew SD, Dirckx SG, Niazy RK, Iannetti GD, Wise RG. EEG signatures of auditory activity correlate with simultaneously recorded fMRI responses in humans. Neuroimage 2010;49:849.

McFarland DJ, McCane LM, David SV, Wolpaw JR. Spatial filter selection for EEG-based communication. Electroencephalogr Clin Neurophysiol 1997;103:386–94.

Middendorf M, McMillan G, Calhoun G, Jones KS. Brain–computer interfaces based on the steady-state visual-evoked response. IEEE Trans Neural Syst Rehabil Eng 2000;8:211–4.

Miranda ER. Plymouth brain–computer music interfacing project: from EEG audio mixers to composition informed by cognitive neuroscience. Int J Arts Tech 2010;3:154–76.

Mouraux A, Iannetti G. Across-trial averaging of event-related EEG responses and beyond. Magn Reson Imaging 2008;26:1041–54.

Müller-Gerking J, Pfurtscheller G, Flyvbjerg H. Designing optimal spatial filters for single-trial EEG classification in a movement task. Clin Neurophysiol 1999;110:787–98.

Müller-Putz GR, Scherer R, Brauneis C, Pfurtscheller G. Steady-state visual evoked potential (SSVEP)-based communication: impact of harmonic frequency components. J Neural Eng 2005;2:123.

Niedermeyer E, Da Silva FL. Electroencephalography: basic principles, clinical applications, and related fields: Lippincott Williams & Wilkins; 2005.

Odom JV, Bach M, Barber C, Brigell M, Marmor MF, Tormene AP, et al. Visual evoked potentials standard (2004). Doc Ophthalmol 2004;108:115–23.

Pires G, Nunes U, Castelo-Branco M. P300 spatial filtering and coherence-based channel selection. 2009 NER'09 4th international IEEE/EMBS conference on neural engineering. IEEE; 2009. p. 311–4.

Popescu F, Fazli S, Badower Y, Blankertz B, Müller K-R. Single trial classification of motor imagination using 6 dry EEG electrodes. PLoS One 2007;2:e637.

Qin L, Ding L, He B. Motor imagery classification by means of source analysis for brain–computer interface applications. J Neural Eng 2004;1:135.

Quian Quiroga R, Garcia H. Single-trial event-related potentials with wavelet denoising. Clin Neurophysiol 2003;114:376–90.

Rakotomamonjy A, Guigue V. BCI competition III: dataset II-ensemble of SVMs for BCI P300 speller. IEEE Trans Biomed Eng 2008;55:1147–54.

Rodgers JL, Nicewander WA. Thirteen ways to look at the correlation coefficient. Am Stat 1988;42:59–66.

Rugg MD, Coles MG. Electrophysiology of mind: event-related brain potentials and cognition. Oxford University Press; 1995.

Scherer R, Muller G, Neuper C, Graimann B, Pfurtscheller G. An asynchronously controlled EEG-based virtual keyboard: improvement of the spelling rate. IEEE Trans Biomed Eng 2004;51:979–84.

Strehl U, Leins U, Goth G, Klinger C, Hinterberger T, Birbaumer N. Self-regulation of slow cortical potentials: A new treatment for children with attention-deficit/hyperactivity disorder. Pediatrics 2006;118:e1530–40.

Su H, Du P, Du Q. Semi-supervised dimensionality reduction using orthogonal projection divergence-based clustering for hyperspectral imagery. Opt Eng 2012;51:111715-1–5-8.

Thomusch O, Sekulla C, Walls G, Machens A, Dralle H. Intraoperative neuromonitoring of surgery for benign goiter. Am J Surg Pathol 2002;183:673–8.

Vaughan TM, Heetderks WJ, Trejo LJ, Rymer WZ, Weinrich M, Moore MM, et al. Brain–computer interface technology: a review of the Second International Meeting. IEEE Trans Neural Syst Rehabil Eng 2003;11:94.

Wang H, Zheng W. Local temporal common spatial patterns for robust single-trial EEG classification. IEEE Trans Neural Syst Rehabil Eng 2008;16:131–9.

Wang Y, Wang R, Gao X, Hong B, Gao S. A practical VEP-based brain–computer interface. IEEE Trans Neural Syst Rehabil Eng 2006;14:234–40.

Wolpaw JR, Birbaumer N, McFarland DJ, Pfurtscheller G, Vaughan TM. Brain–computer interfaces for communication and control. Clin Neurophysiol 2002;113:767–91.

Xu N, Gao X, Hong B, Miao X, Gao S, Yang F. BCI competition 2003-data set IIb: enhancing P300 wave detection using ICA-based subspace projections for BCI applications. IEEE Trans Biomed Eng 2004;51:1067–72.

Zhang H. The optimality of naive Bayes. In: Proceedings of the 17th International FLAIRS conference (FLAIRS2004). AAAI Press; 2004.